Mammal Research (2020) 65:33–48
https://doi.org/10.1007/s13364-019-00455-0

ORIGINAL PAPER

Shrew dentition (Lipotyphla: Soricidae)—endodontic morphology and its phylogenetic resolving power

Leonid L. Voyta[1] · Vladimir S. Zazhigin[2] · Ekaterina A. Petrova[1] · Ludmila Yu. Krjutchkova[3]

Received: 2 July 2019 / Accepted: 22 August 2019 / Published online: 2 September 2019

Abstract

Soricid (Lipotyphla: Soricidae) inner tooth structures have been described for the first time using high-resolution X-ray computed micro-tomography. The endodontic morphology of shrews is complex and according to our results can be used (i) for the description of additional odontological features, (ii) for phylogenetic investigations on a morphological basis, and (iii) for determining the homology of the tooth elements. The results of the original analysis revealed a gradual process of dentine formation and, correspondingly, decreasing pulp volume in immature and mature specimens of *Sorex mirabilis*. However, analysis of the age-related changes also revealed an irregularity in the dentine deposition within different parts of a pulp cavity. We named this irregularity "selective pulp overgrowth". This process was confirmed by the analyses of specimens of *Sorex minutissimus*, *Neomys fodiens* and *Blarina brevicauda*. Attempts to explain selective overgrowth led us to consider the functions of tooth pulp. According to dentistry investigations, one of the several functions of pulp is dentine innervation. We assume that dentine innervation is a significant feature of soricid teeth. A list of twelve characters displays the possible application of pulp endocast morphology to phylogenetic investigations. We suggest that pulp endocast analysis be added to the analysis of the tooth surface to achieve the broadest and most productive use of tooth morphology.

Keywords Odontology · Endodontic morphology · Pulp cavity · Radicular canal · Pulp endocast · Soricidae · Phylogeny · Micro-tomography

Introduction

Soricids (Lipotyphla: Soricidae) have a heterodont dentition that consists of highly specialized first incisors, variable numbers of unicuspid teeth, upper and lower fourth premolars and three molars. Due to the large size of the lower incisor, the lower dentition of Soricidae is highly reduced. Therefore, the upper teeth represent a more useful object for analysing the variety of tooth types or "tooth families" sensu Butler (1981). The upper molars are quadritubercular, and the first two upper molars are the most complex within the dentition. Each tooth type independently consists of crown and root parts. The crown is mostly covered by double-layered enamel (Dumont et al. 2014). Dentine forms the main matter (body) of the tooth. Inside the tooth crown are the pulp chambers. The chambers are filled with pulp, which is soft, vascularized and innervated tissue (Hillson 2005).

Two critical processes, dentinogenesis and amelogenesis, are most significant in tooth development (Hillson 2005; Ungar 2010). Both of these processes gradually form dentine and enamel layers through the production of the odontoblasts and ameloblasts (and other structures such as the predentine and enamel matrices), correspondingly. The histochemical and growth actions upon the enamel-dentine junction (EDJ) determine tooth shape. Ungar (2010: 23) wrote: "Mammalian tooth shape is determined by the patterns of folding and growth of tissues at the interface between the epithelium [enamel producing – LV] and the mesenchyme [dentine and pulp producing – LV] during dental development …". The tooth "pulpal mesenchyme" is involved in dentinogenesis in two ways (sensu Goldberg and Lasfargues 1995: 15): (i) as a superficial layer

Communicated by: Jan M. Wójcik

✉ Leonid L. Voyta
leonid.voyta@zin.ru

[1] Zoological Institute, Russian Academy of Sciences, Universitetskaya nab. 1, St. Petersburg, Russia 199034

[2] Geological Institute, Russian Academy of Sciences, Pyzhevskii per. 7, Moscow, Russia 109017

[3] Saint Petersburg State University, Universitetskaya nab. 7, St. Petersburg, Russia 199034

for odontoblast production and (ii) as a pulp proper. The latter gradually reduces in volume due to the growth of the predentine mass and its mineralisation (Hillson 2005; Ungar 2010). Therefore, the pulp cavity seems more essential and useful for the understanding of a "hidden part" of tooth development in comparison to the "visible part" of the tooth surface. In turn, endodontic morphology, including the shape of the pulp chambers and the canal system, may provide previously underutilized data for phylogeny reconstruction.

The rate of dentine formation and decrease in pulp cavity volume is an important variable in the formation of endodontic morphology. According to Hillson (2005), in many mammals, dentine deposition occurs at a rate of 4 μm per day. Ungar (2010) has clarified that the rate of the process is approximately 2–4 μm per day; it can be up to 16 μm in some mammals. However, the inner tooth morphology of shrews is still undescribed, and many questions remain about the pulp functions and about age-related changes in the pulp cavity. Modern computed micro-tomography (micro-CT) approaches (Borths and Stevens 2017; Keine et al. 2017; Ni et al. 2012; Wu and Schepartz 2009; among others) allow the analysis of "hidden morphological features", including the endodontic morphology of shrew teeth.

The present work represents the first original description of the endodontic morphology (pulp system) of the upper dentition of four species of red-toothed shrews (subfamily Soricinae Fischer, 1817). Our primary objective is a preliminary assessment of the resolving power of endodontic morphology for phylogenetic reconstruction and possibly other applications.

Material and methods

Sampling

The studied material consists of immature (subadult, sad) and mature (adult, ad) specimens of *Sorex mirabilis* Ognev, 1937 and single specimens of *Sorex minutissimus* Zimmermann, 1780 (sad), *Neomys fodiens* (Pennant, 1771) (sad) and *Blarina brevicauda* (Say, 1823) (ad). The right upper toothrows were used for pulp system analysis. A total of five specimens were analysed (Appendix 1). The taxa list was determined in accordance with (i) differences in age stage (sad/ad); (ii) differences in trophic niche/metabolic rate (minute *S. minutissimus* vs large *S. mirabilis* within the genus); (iii) differences in taxonomic position (members of the Soricini/Neomyini/Blarinini tribes). All studied materials are housed in the Scientific Collections of the Zoological Institute, Russian Academy of Sciences (ZIN, St. Petersburg, Russia).

High-resolution X-ray computed micro-tomography

Specimens ZIN 83904 and ZIN 103204 of *S. mirabilis*, ZIN 98582 of *S. minutissimus*, ZIN 75791 of *N. fodiens* and ZIN 65805 of *B. brevicauda* were scanned on the SkyScan 1172 Scanner at the Centre for X-ray Diffraction Studies of Saint Petersburg State University (Saint Petersburg, Russia). The SkyScan settings were as follows: Cu radiation; aluminium filter 0.5 mm; two connected scans in one position; acceleration voltage = 59 Kv (ZIN 98582), 70 kV (ZIN 83904 and ZIN 75791), 80 kV (ZIN 65805 and ZIN 103204); resolution = 5.24 μm (ZIN 65805, ZIN 75791, and ZIN 83904), 6.00 μm (ZIN 103204), 6.48 μm (ZIN 98582); specimen rotation angle = 0.2°; and exposure = 1070 ms (ZIN 65805), 1100 ms (ZIN 75791 and ZIN 98582), 1120 ms (ZIN 83904), 1290 ms (ZIN 103204). All specimens were scanned in three-slice mode. Preliminary processing was performed with DataViewer ver. 1.5.4.0 (SkyScan, Brucker).

Pulp cavity segmentation

Each studied specimen was presented as the image volume. The main processing of the tooth structure (3D digital reconstruction, surface rendering and measurements) was performed using Amira ver. 5.4.3 (VSG). While the image volume preparation of each tooth, we detected at least three patterns: enamel, as the lightest pattern; dentine, presented by the darker than enamel's pattern; and pulp cavity, as the dark-grey or black pattern. The 3D reconstruction of the outer and inner tooth structures performed for the hard tissues (i.e. together for enamel and dentine) and the "soft tissues" (i.e. pulp cavity).

Anatomical directions

Our descriptions of the dentition used standard anatomical directions such as buccal/lingual, anterior/posterior (Ungar 2010) and occlusal (coronal)/apical (Hillson 2005). However, for description of the relative position of the tooth elements, it was necessary to use "reversed" terms to correspond to the reversed view seen by a zoologist who views the upper teeth through a microscope. In the natural position of an upper premolar, for instance, the tip of the paracone is situated lower than the tip of the parastyle. In reversed view, it was necessary to use the opposite comparative adjective—"higher" (as it appeared to the zoologist's eye) (see details and explanations in Appendix 2 in Fig. 8).

Results

Endodontic morphology—short description

The dental pulp is the soft connective tissue within the pulp cavity, including odontoblasts, nerve fibres and blood vessels (Ungar 2010). The inner pulpal system of the soricid tooth has a complex three-dimensional shape that is formed by the coronal cavity and canals, including the radicular canals. The common pulp chamber is a cavity within the coronal portion of a tooth

(Pashley et al. 2002). Several local chambers of various sizes are positioned within the main cone matter of the shrew tooth. The tooth surface nomenclature follows that of Lopatin (2006: 212). However, to make it easier to use abbreviations of the main cones and their corresponding pulp chambers, we used upper case for abbreviations of surface structures (MC, metacone; PC, paracone; ENC, entocingulum; ABR, anterobuccal root; etc.) and lower case for endodontic structures with the addition of the letters: "h" (as "chamber") for the cavities, "x" (as "extension") for the extensions and "c" (as "canal") for coronal and radicular pulpal canals.

The first upper molar possesses four local cavities, including the metacone (mch), the paracone (pch), the protocone (prch) and the hypocone (hch) chambers, descending in size (Figs. 1 and 2). Each cavity forms and retains a pointed portion, the so-called pulp horn, which is closely associated with the innervation of the coronal dentine (Pashley et al. 2002). The "stylar shelf" (see Jernvall 1995: 6) of a shrew molar is well developed and bears three styles: the parastyle (PST), the mesostyle (MSS) and the metastyle (MST). The inner portions of the styles have more or less developed pulpal extensions, the parastyle (pstx), mesostyle (mssx) and metastyle (mstx) extensions (Fig. 2). The hypoconal flange of molariform teeth often has a distinct hypocone and "hypoconal flange ridge" (HFRG) that bear the pulpal canal of an entocingulum (encc; *syn*. a canal of the hypoconal flange ridge). The ectocingulum also has a corresponding pulp canal (ecc). The number of radicular canals (*syn*. pulp/pulpal canal of roots) corresponds to the number of main roots: the anterobuccal root (ABR) of M1 and the radicular canal of the anterobuccal root (arbc), the posterobuccal root (PBR) and its radicular canal (pbrc); the anterolingual root (ALR) and its canal (alrc); and the hypoconal flange root (HFR) and its canal (hfrc). Each root terminates at the apical foramen, which can be "open" on the main roots and may be "closed" with age on reduced ("unstable") roots. Below, we describe the 3D reconstruction of the pulpal endocast of the upper dentition of shrews in formal terms.

Changes in the pulp chamber with age

Pulp cavity size and volume gradually decrease with age due to the formation of dentin (Pashley et al. 2002). Hillson (2005: 188) stated, "[…] dentine formation continues slowly inside

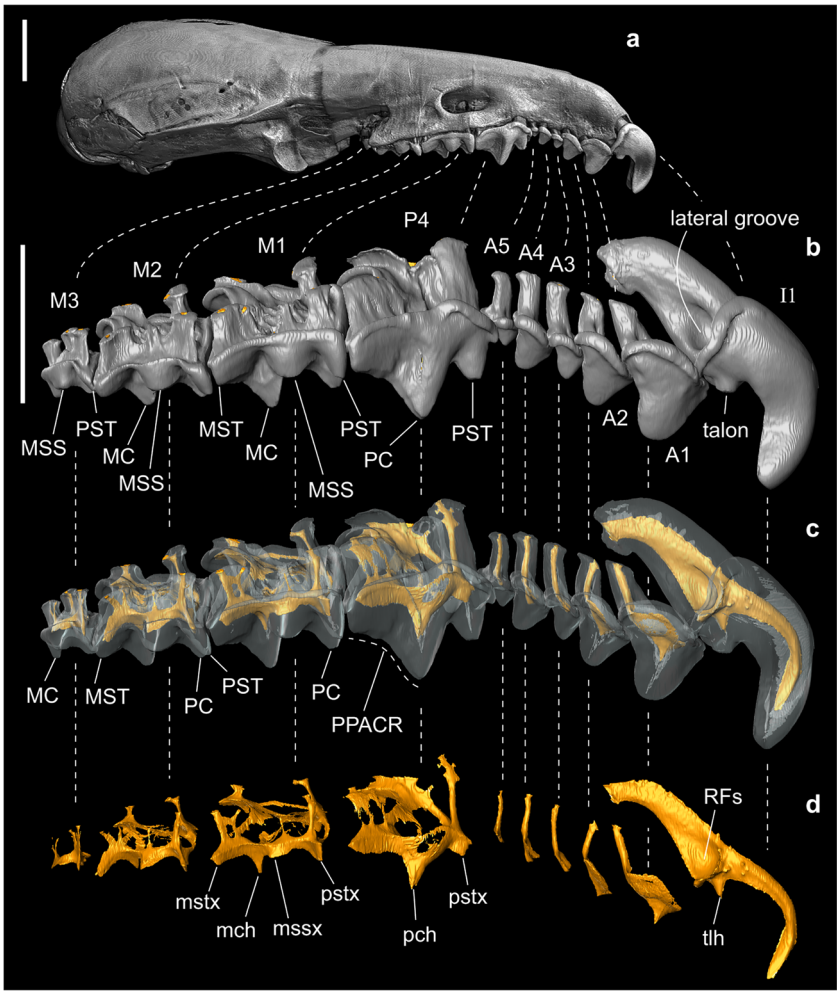

Fig. 1 *Sorex mirabilis* (ZIN 83904) skull and upper tooth-row in lateral view. (a) Skull, scanned surface view. (b) Upper dentition three-dimension model. (c) Upper dentition three-dimension model, transparent view. (d) Pulp endocast three-dimension model. All scale bars represent 1 mm. An upper antemolars (first–fifth), I1 first upper incisor, Mn upper molars (first–third), MC metacone, mch metacone pulp chamber, MSS mesostyle, MST metastyle, mstx metastyle pulp extension, P4 fourth upper premolar, pch paracone pulp chamber, PC paracone, PPACR postparacrista (dotted line), PST parastyle, pstx parastyle pulp extension, RFs "radicular fossa" (see text), tlh talon pulp chamber

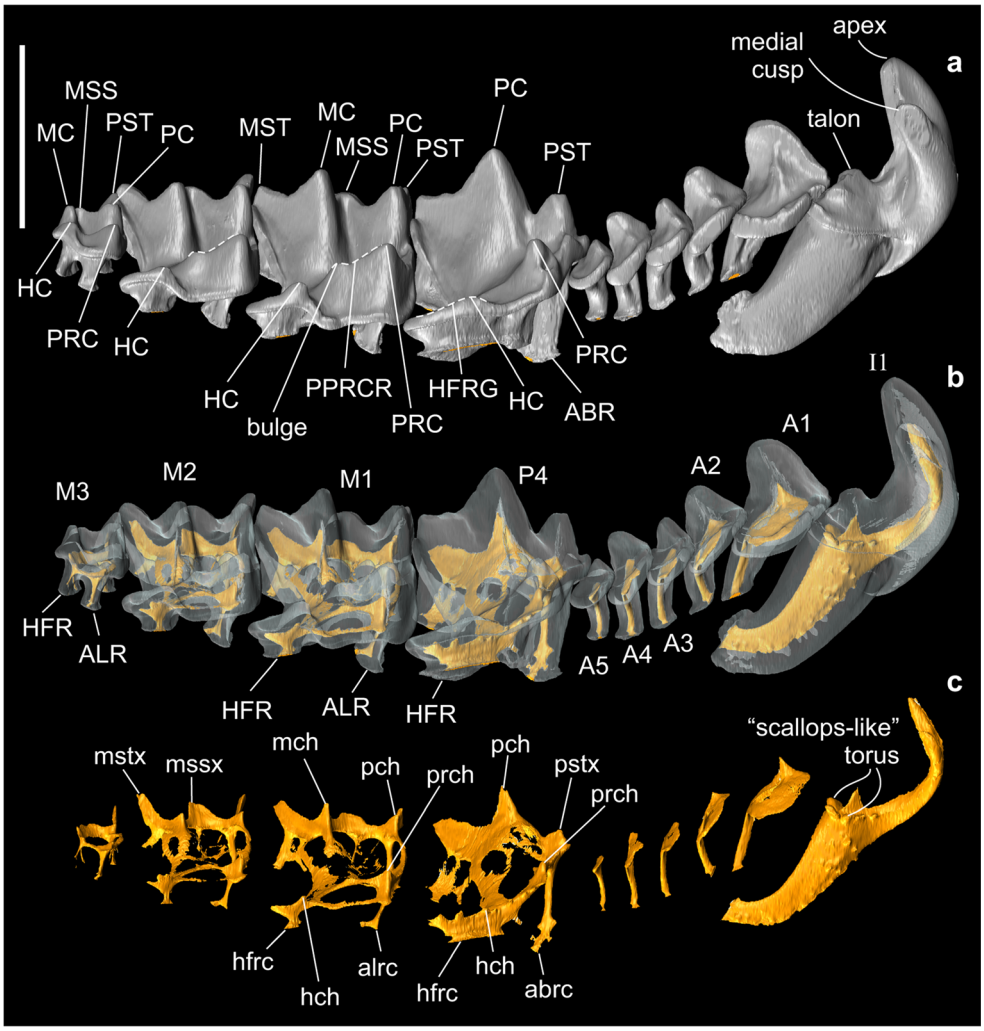

Fig. 2 *Sorex mirabilis* (ZIN 83904) upper tooth-row in lingual view. (a) Upper dentition three-dimension model. (b) Upper dentition three-dimension model, transparent view. (c) Pulp endocast three-dimension model. Scale bar represents 1 mm. ABR anterobuccal root, abrc pulpal canal of ABR, ALR anterolingual root, alrc pulpal canal of ALR, HC hypocone, hch hypocone pulp chamber, HFR hypoconal flange root, hfrc pulpal canal of HFR, HFRG hypoconal flange ridge (dotted line), PPRCR postprotocrista (dotted line); also see Fig. 1

the completed parts of the pulp chamber and root canal. Odontoblasts remain active and layers of secondary dentine are continuously deposited, lining the pulp chamber walls". The process may vary among different groups of shrews and, if so, it is likely to be related to body size, metabolic rate and phylogenetic affinity.

Sorex mirabilis

Large shrew (CI = 22.5–24.2 mm). Endemic species with extremely narrow geographical range within the Palearctic. Inhabits primary broad-leaved and broad-leaved/coniferous forests of the Far East (Zaitsev et al. 2014).

Occlusal surface condition

Teeth of the immature specimen (ZIN 83904) unworn. The occlusal surface of P4 is devoid of wear facets (Fig. 3: a1, a2). The mature specimen (ZIN 103204) displays heavily worn teeth with broad wear surfaces (Fig. 3: b1, b2). Accordingly, the first specimen was determined as "subadult" (= unworn teeth) in terms of "relative age group"; the second specimen was determined as "adult 2" (heavily worn teeth) (Fig. 3).

Pulpal endocasts of an immature specimen

The first upper incisor bears a developed, curved pulp cavity within a relatively long part of the apex, the well-developed extension of a medial cusp and a cone-like pulp chamber of a talon (Figs. 1, 2 and 4: a). The coronal part of an endocast is separated from the radicular part by a scallops-like torus and the "radicular fossa" (RFs). This fossa corresponds to the lateral groove of the root. The radicular canal is flattened and wide in its precoronal ("precervical") part and gradually narrows and curves towards the broad apical foramen (Fig. 1: d).

Antemolars (Fig. 5: a1, a2): A1 displays a high, pointed pulp horn. The pulpal canal of the posterocrista (*syn*. Central canal) is well developed and slightly curved in the middle part towards the buccal side. The "buccal lobe" of the chamber presents a relatively narrow, fully closed ectocingulum pulpal canal (*syn*. ectocingular canal) that is separated from the canal of the posterocrista by a suboval broad "fenestra" (i.e., an area

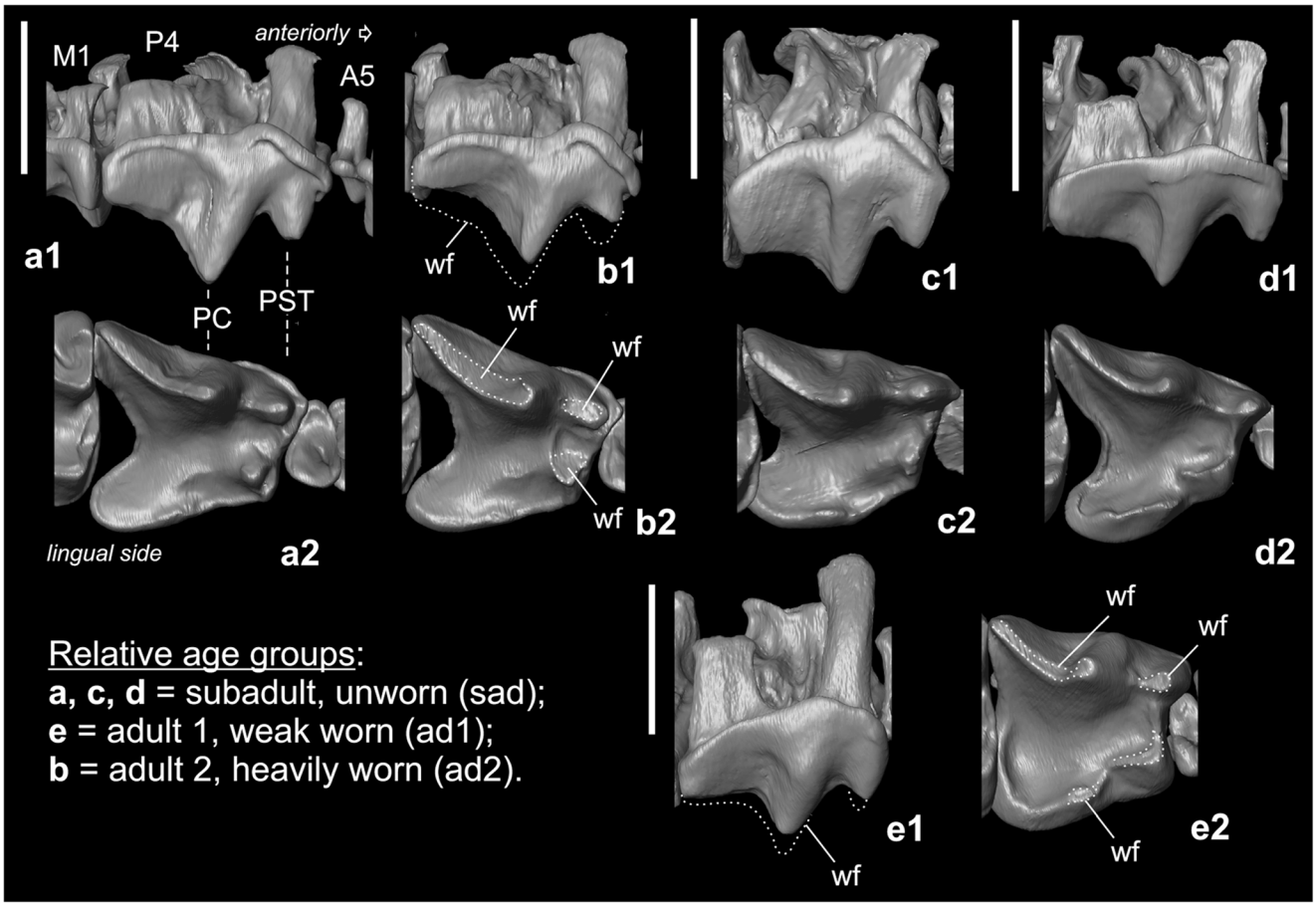

Fig. 3 Fourth upper premolar of *Sorex mirabilis* (ZIN 83904 (a); ZIN 103204 (b)), *S. minutissimus* (ZIN 98582 (c)), *Neomys fodiens* (ZIN 75791 (d)) and *Blarina brevicauda* (ZIN 65805, e): *n*1, P4 in buccal view. *n*2, P4 in occlusal view. Scale bars represent 1 mm (a, b, d, e); 0.5 mm (c). wf wear facet (white dotted line); also see Fig. 1

with deposited dentine). The "lingual lobe" of the chamber similarly presents an entocingulum pulp canal (*syn*. entocingular canal) that is broader than the ectocingular canal and is separated from the central canal by the fenestra. Undoubtedly, the earlier stage of pulp chamber development presents whole lobes without fenestrae. A2 displays similar conditions to A1 but has a smaller pulp horn. The buccal lobe is whole, without fenestrae. The lingual lobe is similar to A1 state but has a narrower entocingular canal. A3 lacks a protruded pulp horn. The buccal lobe is weakly developed. The lingual lobe is developed with small netted fenestrae. The chamber of A4 is larger than the chamber of A3 according to the difference in the tooth size (Figs. 1: b and 2: a). A4 has a weakly developed pulp horn and a weakly expressed buccal lobe like the short process (buccal process). The lingual lobe is broad; the anterior half of the entocingular canal is broad, and the posterior half is narrower. The lobe bears round fenestrae. The chamber of A5 is small and spatula-like with a small buccal process. The position of the central canal is uncertain; the lingual lobe is weakly developed. The radicular canals of the antemolars are well developed.

The fourth upper premolar (Figs. 1: d and 2: c) bears a high and pointed pulp horn of the paracone chamber. The developed pulpal canal of the postparacrista extends from the paracone chamber to the posterobuccal corner and ends in a pointed tip. In the base of the canal lie buccal and posteromedial toruses that mark the position of the ectocingulum and posterocingulum, respectively. In the base of the paracone chamber lies the canal of the ectocingulum. The extension of the parastyle is developed into a high and narrow ridge. The protocone pulp chamber is weakly developed and appears as a low bulge. The "lobe" of the hypoconal flange chamber presents a "net-like" dentine field and the entocingular canal with multiple "temporal extensions" along its occlusal side. The size of these extensions allows supposing that the "hypocone chamber" is among them, but further analysis of the mature specimen reveals the temporal nature of the extensions and the absence of the expressed hypocone chamber (see below). The "bypass canal" connects the parastyle extension with the protocone bulge and the lobe of the hypoconal flange. P4 has three radicular canals: the long and developed anterobuccal canal, the posterobuccal "friable"

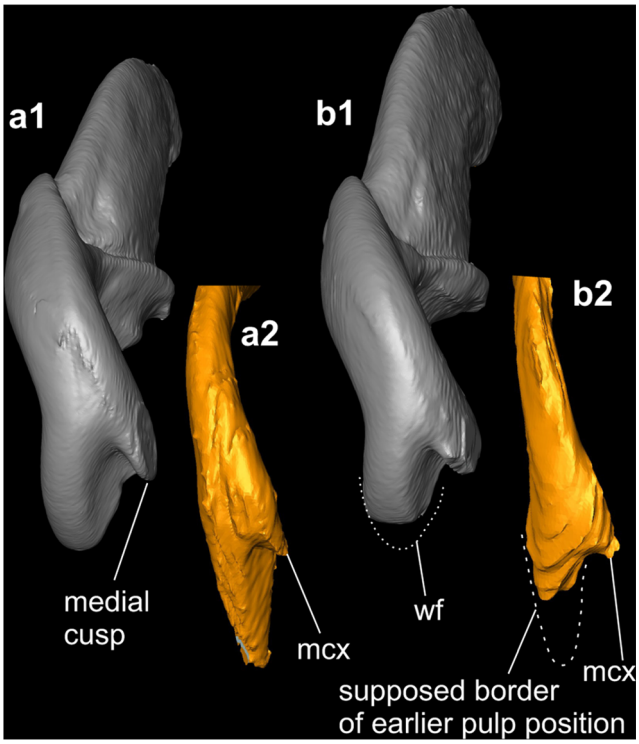

Fig. 4 *Sorex mirabilis* (ZIN 83904 (a); ZIN 103204 (b)) first upper incisor and partly pulp endocast of I1 tip: (a1, b1) I1 in frontal view. (a2, b2) Tip of I1 pulp endocast. Unscaled. mcx medial cusp pulpal extension; also see Figs. 2 and 3

canal with two wide longitudinal gaps and the broad, very short radicular canal of the hypoconal flange.

First upper molar (Figs. 1: d and 2: c) has M1 has the highest pulp horn of the metacone chamber and closely repeats the metacone shape with its pre- and postmetacrista. The pulp horn of the paracone chamber is noticeably lower than the metacone horn. The parastyle extension is well developed and presents a sharp ridge with a protruded pointed tip of pulp horn. The mesostyle extension is broad, flattened and well protruded upward. The metastyle extension is weakly protruded upward relative to the upper ridge of the postmetacristal pulp canal. The protocone chamber forms a well-protruded triangular pyramid with the pointed tip of the horn. The canals of the preprotocrista and postprotocrista are well developed. The hypocone pulp chamber presents a pointed pulp horn that protrudes upward relative to the short entocingular canal. The pulp horn is flattened along the canal axis. The four radicular canals are well developed. M1 has the anterolingual radicular canal, which is stable with age, below the protocone chamber and the short and narrow canal of the hypoconal flange. The friable posterobuccal radicular canal of M1 displays a similar condition to P4. The M2 pulpal system displays similar conditions to M1 with several noticeable differences: (i) the metacone pulp chamber of M2 is similar to the paracone chamber in the size and height of the pulp horns; (ii) the pulpal lobe of the stylar shelf is more developed in M2 due to changes in occlusal morphology and significant shifts (buccally and occlusially) of the parastyle and mesostyle relative to the paracone and metacone tips. The M3 pulp chamber is characterized by weak protrusion of the pulp horns of the cones and styles. The paracone chamber presents a low and blunt horn. The metacone chamber is flattened and protrudes weakly upward to the edge of the short canal of the premetacrista. The visible notch of the arched canal that connects the metacone and paracone is a possible mark of the "split" mesostyle pulp extension (similar to the split mesostyle and its pulp extension of M1–M2 in *Blarina*; see below). The hypocone chamber is blunt and very weakly visible. The protocone pulp chamber is developed to a degree similar to that of the paracone chamber or slightly weaker. The anterobuccal radicular canal is the most developed; the anterolingual canal is stable but slightly weaker than the former. The unique condition of the M3 of *S. mirabilis* is the retention of two posterior radicular canals, the posterobuccal root canal and the radicular canal of the hypoconal flange. These canals are short, very weakly developed and narrow in diameter, but they undoubtedly mark the metacone and the hypocone. The posterobuccal canal is unstable with age (see below for a description of the mature specimen).

Pulpal endocasts of a mature specimen (stage ad2)

The first upper incisor (Fig. 4: b1, b2) displays visible reduction of the pulp endocast volume compared to the immature specimen, but despite the advanced age (ad2) of the specimen, the coronal and radicular parts of the endocast are still broad. The radicular canal has lost approximately two-thirds of its "height" (in lateral view). The central part of the radicular fossa is filled with dentine and retains only a narrow canal in its lower part. The pulp chamber of the talon is not distinct. The cervical part retains a weak torus with a slightly extruded rare extension. The anterior end of the crown attracts attention due to the irregularity of a more rapid decrease in the apex part and a slower decrease in the medial cusp pulp extension (Fig. 4: b2).

The antemolars display visibly decreased pulp endocast volume (Fig. 5: b1, b2). The pulp horns of A1–A2 and A4 become blunt. The lingual pulp lobe has decreased to the narrow entocingular canal with gaps. The buccal lobe has decreased more than the opposite lobe; A1–A2 display a weak ectocingular canal with a broad gap in its anterior part, whereas A3–A5 display only the buccal processes instead of the ectocingular canals. All radicular canals are of sufficient diameter to ensure pulp health.

The fourth upper premolar (Fig. 6: a) displays more or less even decreases in the expression/height of the paracone chamber and the parastyle extension. The weak protocone chamber (bulge) almost did not change its state. The hypocone chamber is slightly distinct and protrudes weakly. In the central part of the coronal cavity and within the hypoconal flange, dentine is deposited in broad fields. The anterobuccal root canal and the canal of the hypoconal flange retain relatively wide diameter,

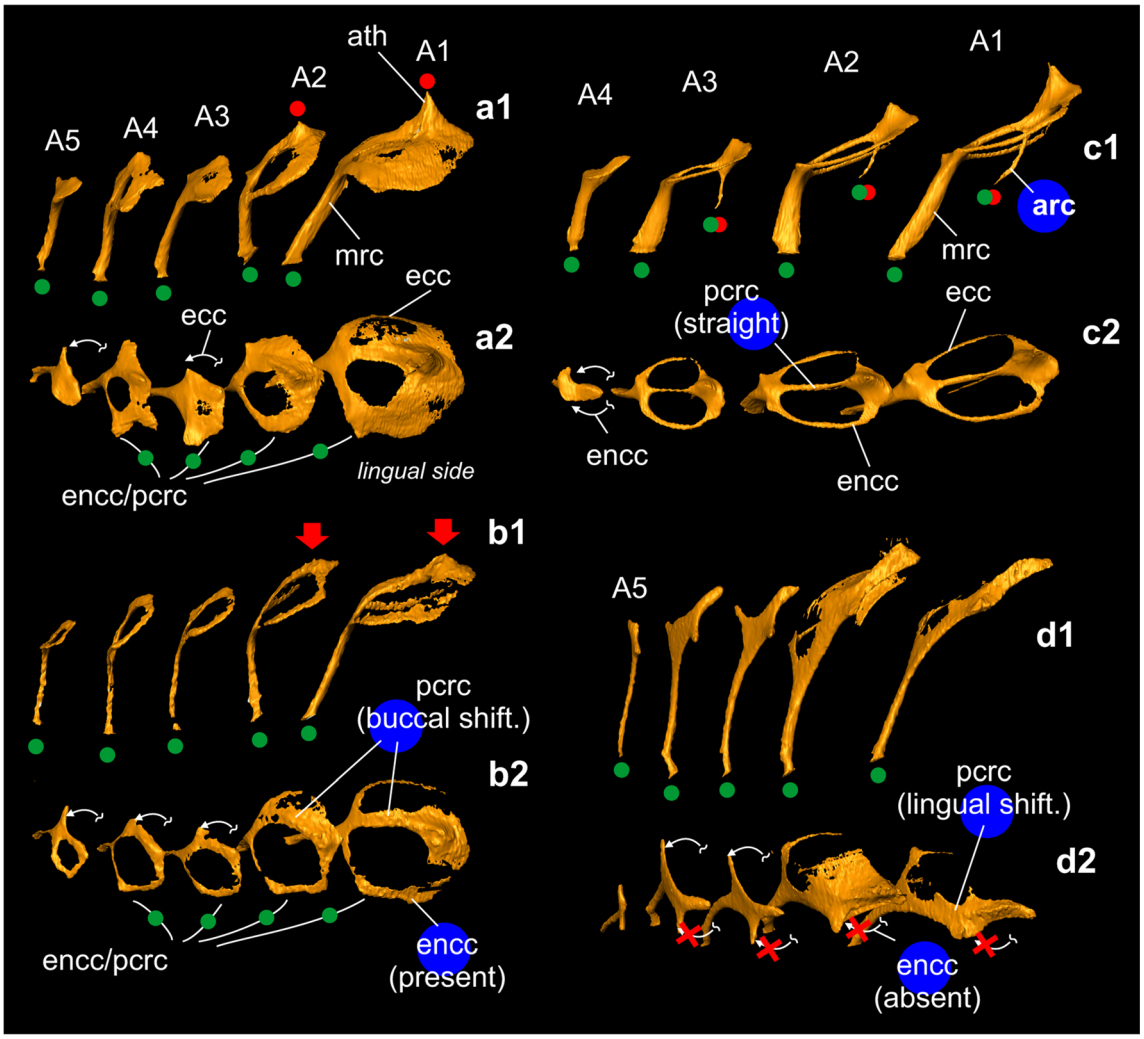

Fig. 5 Pulp endocast three-dimension model of antemolar row of *Sorex mirabilis* (ZIN 83904 (a); ZIN 103204 (b)), *Neomys fodiens* (ZIN 75791 (c)) and *Blarina brevicauda* (ZIN 65805 (d)): *n*1, antemolars in lingual view. *n*2, antemolars in occlusal view. Unscaled. arc anterior radicular canal, ath antemolar chamber, ecc ectocingulum pulpal canal, encc entocingulum pulpal canal, mrc main radicular canal, pcrc posterocrista pulpal canal; blue circle age-independent significant differences in pulp structures; green point shows non-overgrowth radicular canal/apical foramen is open, or non-reduced canals (see details in text); green + red points—uncertainty for overgrowing of a root canal/apical foramen to the ad2/senile stage; red arrow—the pulp chamber volume decreases with age; red cross—initial absent of encc (see D2, evolutionary reduction); red point—an initial condition of the pulp chamber (see red arrow as opposite state); white arrows—supposed position of a reduced ecc or/and encc, corresponding to side (i.e. age-related or evolutionary reduction); also see Fig. 1

but the posterobuccal radicular canal has lost passability and is reduced to three narrow closed/blind canals.

M1–M2 (Fig. 6: a) clearly display the direction in which pulp volume decreases, which is from the occlusal part to the precervical part or rather from the outer layers into the pulp cavity. Thus, the central part of the coronal chamber is fully overgrown, but all significant elements retain their functionality, including the bypass pulp canal (possibly the canal of the anterocingulum), the canals of the stylar shelf, the entocingular canal and the distinct chambers of the metacone, paracone, protocone and hypocone. Here is repeated the "irregularity" of the decrease in pulp volume, as was mentioned for the first incisor (see above). All four radicular canals of M1–M2 are retained in an open state with moderate decreases in diameter. M3 has all functional canals without protruded chambers and only three open radicular canals: the anterobuccal canal, the anterolingual canal and the canal of the hypoconal flange. The posterobuccal radicular canal is fully reduced.

Endodontic morphology of some soricine shrews

Sorex minutissimus

Minute shrew (CI = 11.7–14.5 mm). Species with a broad geographical range within the Palaearctic. Inhabits different types of intermediate (ecotonal) habitats, for instance, on the borders of forests or swamps. Quite often found in disturbed poor habitats (Zaitsev et al. 2014).

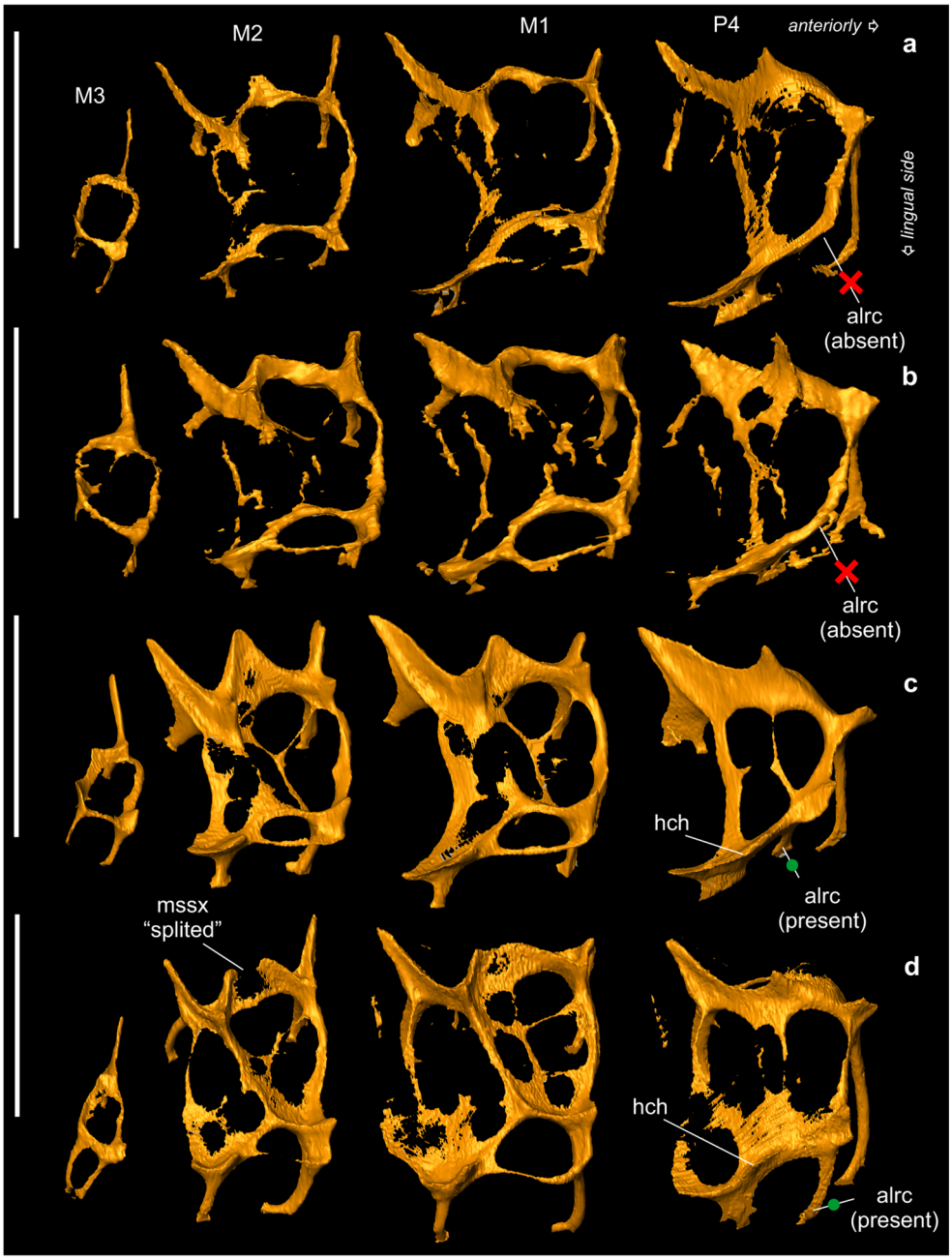

Fig. 6 Pulp endocast three-dimension model of the molariform teeth of *Sorex mirabilis* (ZIN 103204 (a)), *S. minutissimus* (ZIN 98582 (b)), *Neomys fodiens* (ZIN 75791 (c)), and *Blarina brevicauda* (ZIN 65805 (d)). Scale bars represent 1 mm (a, c, d) and 0.5 mm (b). Abbreviations: see in Figs. 1, 2 and 5 and explanations in the main text

Occlusal surface condition

Teeth of the immature specimen (ZIN 98582) fully unworn (Fig. 3: c1, c2). The specimen was assigned to the relative age group "subadult".

Pulpal endocasts of an immature specimen

The first upper incisor of the immature specimen (Fig. 7: a) displays the lowest volume of the coronal pulp chamber in relation to mineralised tooth tissues, enamel and dentine compared to other analysed specimens, including mature individuals of *B. brevicauda* (stage ad1) (Fig. 7: c) and *S. mirabilis* (stage ad2) (Fig. 4: b). In visual relation (see Fig. 7: a in lateral view), the coronal part of the endocast occupies less than half of the tooth crown. The talon chamber is well determined with a pointed pulp horn, but the common volume of the chamber is very reduced relative to the hard tooth matter. The cervical part is indistinct. The radicular canal is similar in diameter to the coronal part but longer than the latter by twofold or slightly more.

The antemolars of the analysed specimen of *S. minutissimus* have coronal cavities that are similar to the cavity of a mature specimen of *S. mirabilis*. The similarity is revealed in the weak expression of the pulp horns (*S. minutissimus* has pointed low horns on A1, A3 and A4), an almost complete reduction of the buccal lobe of the chamber and a partial reduction of the lingual

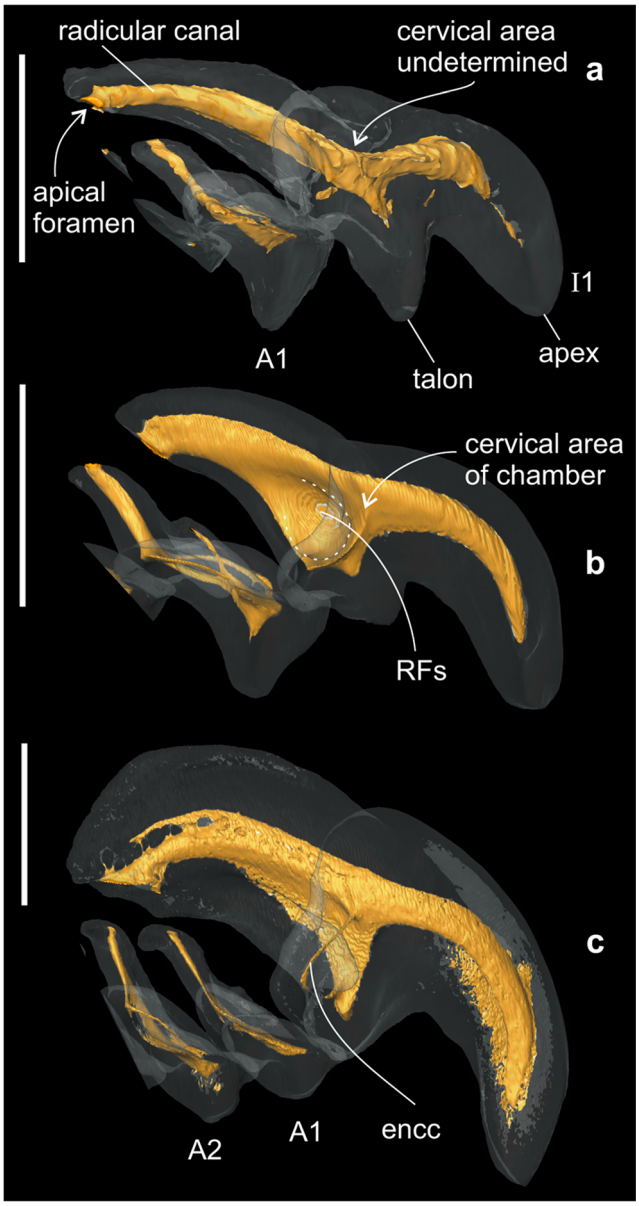

Fig. 7 Upper anterior teeth (I1–A1, A2) three-dimension model in transparent buccal view of *Sorex minutissimus* (ZIN 98582 (a)), *Neomys fodiens* (ZIN 75791 (b)) and *Blarina brevicauda* (ZIN 65805 (c)). Scale bars represent 1 mm (b, c) and 0.5 mm (a). Abbreviations: see in Figs. 1 and 5 and explanations in the main text

lobe with retention of the narrow entocingular canal with gaps. In general, the coronal pulp condition of *S. minutissimus* antemolar teeth seems mature. Oppositely, all radicular canals are well developed according to the relative age stage.

The fourth upper premolar (Fig. 6: b) displays a high, narrow base of the pulp horn of the paracone chamber. The upper ridge of the postparacrista pulp canal is directly opposite these ridges in the other specimens. The parastyle pulp extension is indistinct. The protocone chamber appears as a bulge on the bypass canal with several narrow unordered protrusions towards the lingual side (with slight tilting in the occlusal direction). The entocingular canal is short with a weakly developed hypocone chamber. The anterobuccal radicular canal is well developed, but the posterobuccal canal and the canal of the hypoconal flange are friable.

The first upper molar (Fig. 6: b) displays a moderately developed metacone chamber with a weakly pointed pulp horn. The paracone chamber is more weakly developed than that of the metacone. The canal of the postmetacrista is longest and lacks an expressed extension of the metastyle (state: metastyle absent). The canal of the postparacrista is similar to the canal of the postmetacrista in length or slightly longer, without any expression of the mesostyle extension. The very short canal of the preparacrista ends in the parastyle extension. The low triangular chamber of the protocone connects posteriorly to the broad canal of the postprotocrista. The entocingular canal is short with an expanded end. The chamber of the hypocone is weakly developed and appears as a bulge. The radicular canals are narrow. The radicular canal of the hypoconal flange is the shortest and displays a waist in the middle part. Compared to M1, M2 has equally low chambers of the metacone and paracone and more developed elements of the stylar shelf. The stylar shelf bears a moderately expressed mesostyle pulp extension and a relatively long preparacristal canal, but the latter lacks a parastyle extension. The chamber of the protocone and the elements of the hypoconal flange lobe are less developed than in M1. The conditions of the radicular canals of M2 are similar to those of M1. M3 has all the functional canals of the coronal cavity. The paracone and protocone chambers are defined as the small extensions at the corresponding places. The anterobuccal and anterolingual radicular canals are similar in size. The radicular canal of the hypoconal flange is reduced and closed.

Neomys fodiens

Large shrew (CI = 19.8–23.6 mm) with a broad geographical range within the Palaearctic. It has a semi-aquatic lifestyle. Inhabits different types of near-water and wet habitats with access to streams and lakes (Zaitsev et al. 2014).

Occlusal surface condition

Teeth of the immature specimen (ZIN 75791) fully unworn (Fig. 3: d1, d2). The specimen was assigned to the relative age group “subadult”.

Pulpal endocasts of an immature specimen

The first upper incisor (Fig. 7: b) displays a long curved coronal pulp chamber without development of the medial cusp pulp extension, despite the presence of a small medial cusp on the occlusal surface. The pulp chamber of the talon displays a cone-like shape with a pointed horn. The cervical area is well

determined by the ridge of the ectocingular pulp canal, and the contour of the radicular fossa is clearly drawn. The radicular canal is wide and slightly shorter than the coronal part.

Antemolars A1–A3 display clear contours of coronal elements (Fig. 5: c1, c2): pointed cone-like pulp horns, a distinct and straight central canal and narrow ectocingular and entocingular canals. The pulp chamber of A4 is reduced in size and has a small buccal process (similar to A5 of an immature specimen of *S. mirabilis*). The radicular part of A1–A3 is relatively complex and bears two broadly separated canals, the main radicular canal (common in other analysed specimens) and the anterior radicular canal. The main canals are well developed and display wide diameters. The anterior canals are shorter than the main canals and display narrow diameters. They probably become closed with age. A4 has no anterior root or corresponding radicular canal.

The fourth upper premolar (Fig. 6: c) displays a high paracone chamber with a pointed pulp horn. The pulp extension of the parastyle presents by its triangular pulp horn. The protocone chamber protrudes far above the bypass canal and bears a weak ridge (canal) that corresponds to the postprotocrista of an occlusal surface. The hypoconal flange displays a relatively long entocingular canal with a high upper ridge and an expressed chamber of the hypocone. The radicular part of the endocast has four distinct canals: the longest, the anterobuccal canal; the wide posterobuccal canal, which is intermediate in size and has a doubled apical end; the short and wide canal of the hypoconal flange; and the anterolingual canal. The last is situated posterior to the protocone chamber and is narrow in diameter with an expanded apical end.

The M1–M2 pulp endocast (Fig. 6: c) clearly corresponds to the occlusal surface of the teeth. Thus, the pulp chambers display well-developed, sharp pulp horns. The mesostyle extension presents as a single protruded element among the elements of the stylar lobe. The parastyle and metastyle extension are not expressed. The radicular part displays four well-developed main canals and one additional temporary canal that is positioned on M1–M2 between the antero- and posterobuccal radicular canals. The M3 cavity displays distinct paracone and protocone chambers, the flattened extension of the mesostyle, and the flattened extension of the metacone (determined by the rudiment of the posterobuccal radicular canal). No chamber or extension of the hypocone is expressed, but the radicular canal of the hypoconal flange is well developed, as are the anterobuccal and anterolingual canals. The posterobuccal canal is present as a rudiment. The presence of all root canals allows identification of the smoothed coronal elements—the metacone and hypocone chambers of M3.

Blarina brevicauda

Large shrew (CI = 20.2–24.7 mm). Species with a broad geographical range within the Nearctic, where it is found in deciduous and coniferous forests and open habitats (Hill and Kelson 1959).

Occlusal surface condition

The teeth of the mature specimen (ZIN 65805) display moderate wear surfaces (Fig. 3: e1, e2). The specimen was assigned to the relative age group "adult 1" (weak worn teeth).

Pulpal endocasts of a mature specimen (stage ad1)

The first upper incisor (Fig. 7: c) bears a large volume of pulpal endocast. Despite the age stage, the tip of the coronal pulp chamber is located close to the occlusal surface (irregular overgrowth, see above). The talon chamber is short and still distinct, with a broad tip. The cervical area is well determined by the narrow and unclosed canal of the ectocingulum. The radicular fossa displays a proportion unlike those of the other analysed taxa, probably due to age-related changes. The radicular canal is broad and bears a wide apical foramen.

The antemolars (Fig. 5: d1, d2) display the indistinct pulp horns of A1–A2 that are presented by bulges (the bulge of A2 is more expressed). The central pulp canal of the posterocrista is well developed on A1–A4 and curves towards the lingual side. The lingual lobe of the A1–A2 pulp chambers is very weak. The weak lingual lobe (and the supposed absence of entocingular canals) is probably a specific character of *B. brevicauda*. In general, the lingual pulpal lobe presents a short lingual process that is better developed on A3–A4 than on A2 and especially on A1. In contrast, the buccal lobes are more developed. The ectocingular canals of the buccal lobes of A1–A2 are relatively long and narrow and are unclosed (with gaps). This lobe of A2 has a wide dentine-free area. A3–A4 display moderately developed buccal processes. The radicular canals of A1–A4 are of sufficient diameter to ensure pulp health. A5 displays a reduced pulp chamber with weakly expressed processes of both the buccal and lingual pulpal lobes and a narrow, open radicular canal.

The fourth upper premolar of a mature specimen (Fig. 6: d), despite the age stage, displays very distinct and well-defined elements of the coronal pulp chamber. The pulp horns of the paracone, protocone and hypocone chambers and the parastyle extension are clearly pointed. The protocone chamber bears a weak ridge (canal) that corresponds to the postprotocrista of an occlusal surface. The hypoconal flange lobe displays net-like dentine fields. The entocingular canal is long and continues as the thin canal of the posterocingulum. The radicular part has four well-developed canals. The anterobuccal canal is longest and has a slightly curved apical end; the posterobuccal and anterolingual canals are similar in size and diameter, and the last canal is situated directly under the protocone chamber. The radicular canal of the hypoconal flange is relatively long and slender.

The M1–M2 pulp endocast (Fig. 6: d) was more complex than those of the analysed immature and mature specimens. The molars of *B. brevicauda* retain a large volume of the pulp endocast with age. Additional significant characters of M1–M2 are the following: (i) pointed pulp horns of all cones; (ii) mesostyle extension absent due to a split of the mesostyle (the postparacrista and premetacrista are not connected); (iii) the canal of the postprotocrista continues by the canal of the metaloph with a bulge that can be interpreted as the metaconule extension and connects with the base of the metacone chamber; (iv) retention of the narrow unclosed canal of the postcingulum. The endocast of M3 is reduced in size and anteroposteriorly compressed corresponding to the condition of the tooth. Within the coronal part are expressed the chambers of the paracone and the protocone only. The radicular part displays equally developed anterobuccal and posterolingual canals and canal of the hypoconal flange. The latter two canals are fused at their apical ends.

Discussion

General remarks

Our investigation of the endodontic morphology of shrew teeth reveals their complexity and demonstrates the occurrence of ambiguous/nonlinear age-related processes. To date, the inner portion of mammalian teeth has been of a subject of interest in studies of the ageing process, and attempts have been made to identify age-diagnostic features (e.g., Tumlinson and McDaniel 1984; Klevesal 2007; Meachen-Samuels and Binder 2009) following successful medical research (Woods et al. 1990; Morse et al. 1991; Indra et al. 2015; among others). Other such studies have focused on specific areas of zoology, for instance, tooth homology (Nweeia et al. 2012). The greatest interest is focused on gaining fundamental (Goldberg and Lastfargues 1995; Byers and Närhi 1999; Pashley et al. 2002) and practical (Goldberg and Smith 2004) information on diseases of the endodont. Shrew endodontic morphology has not been described because this group of mammals is not of interest to the medical and veterinary fields. Therefore, we attempted to determine the possible applications of shrew endodontic morphology and its limitations in the purely zoological field. A comparison of immature and mature specimens of *S. mirabilis* shows that the pulp volume decreases during the gradual process of dentine formation with age. This was expected. However, the observed irregularity in the deposition of dentine within different parts of the pulp cavity was unexpected. This irregularity was observed in the pulp chamber of the first upper incisors of *S. mirabilis* (Fig. 4); as the animal aged, dentine was deposited in the cavity of the apex, but almost no dentine was deposited in the cavity of the medial cusp. Further comparisons of various upper teeth of immature and mature shrews confirmed the presence of an irregularity in pulp chamber overgrowth specifically in the pulp chambers of the cones (e.g., the metacone and paracone chambers of M1–M2 of mature *S. mirabilis*) and canals (canals of the stylar shelf, the bypass canal, and the radicular canals of mature *S. mirabilis*). It is likely that the "selective overgrowth" of the pulp cavity parts is determined by their specific functions.

Functions of pulp and pulpal chambers

According to Ungar (2010: 20), the dental pulp contains blood vessels and nerve fibres. It receives extensive sensory innervation. Dentistry studies describe several functions of inner pulpal innervation, including (i) integration of regulatory mechanisms during tooth development, (ii) reaction to inflammation of the tooth tissues, (iii) initiation of immune and healing responses in tooth tissues and (iv) sensitivity to many types of stimulation (mechanical, chemical, thermal) (Byers and Närhi 1999; Luukko and Kettunen 2016). Thus, pulpal innervation is significant for the "normal" development of the dental crown and the whole tooth and further supports the essential reactions of the living tooth through different types of sensitivity. The sensitivity is determined by the number of sensory nerve endings located in the soft pulp and dentine. What happens when innervation is lost, for example after pulp overgrowth? Byers and Närhi (1999: 16) reported that partially or complete denervated teeth may exhibit impaired pulpal healing. This observation suggests that open pulpal chambers and canals support the innervation and nutrition of living tissues. However, according to Ungar (2010: 20), pulp gradually "becomes more fibrous and less vascular over time". Shrews likely undergo a rapid decrease in pulp volume due to their high rate of metabolism (Taylor 1998). Nevertheless, the current study reveals (i) the retention of a relatively large volume of the pulp cavity with age, including the retention of sufficient diameter of the radicular canals/apical foramina to ensure pulp health and (ii) the selective overgrowth of the pulp cavities. Therefore, the more likely reason for the "open canals" is probably related to the function of mechanical sensitivity of the teeth through innervation. Byers and Närhi (1999: 15) stated: "… fast-conducting, vibration-sensitive intrapulpal fibres may be involved in special occlusal sensitivity". Dong et al. (1993) studied the significance of periodontal ligament mechanoreceptors and intradental mechanoreceptors in determining the tactile sensibility of teeth. Using the example of a cat canine tooth, the authors showed that both types of mechanoreceptor provide occlusal sensitivity. The authors speculated that the tactile sensibility of teeth can be important for "protecting the structural integrity of tooth enamel from severe abrasion or percussion during an activity such as biting, grasping, or gnawing and for signalling the texture of food during mastication" (Dong et al. 1993: 1580). Based on the results obtained by Dötsch (1986, 1994) in electromyographic and cinematographic studies of shrew masticatory activity

(chewing sequences) and on the complexity of the occlusal surfaces of shrew teeth (see details in Zazhigin and Voyta 2019), we assume that there is a real need for the tactile sensibility of shrew dentition. During different types of grasping and chewing actions, the shrew must sense pressures, forces, prey resistance, etc. Accordingly, one of the important functions of the living pulp in soricids is the provision of dental sensitivity. The need for this function can determine the rate of dentine formation and the selection of places for its deposition. Thus, the chamber volumes and radicular canals remain open despite the high rate of shrew metabolism.

However, immature specimens of *S. mirabilis*, *S. minutissimus* and *N. fodiens* displayed varying tooth hard matter/pulp volume ratios. For instance, the distance between the anterior end of the I1 pulp chamber and the anterior end of the occlusal surface of I1 is longer in *S. minutissimus* (Fig. 7: a) than in *S. mirabilis* (Fig. 1: d), *N. fodiens* (Fig. 7: b) and even in mature *B. brevicauda* (Fig. 7: c). Here, we need to return to the question of occlusal sensitivity. Byers and Närhi (1999) discuss two views of occlusal sensitivity: (i) the theory of "periodontal sensitivity" proposed by Linden and Millar (1988) and (ii) the theory of "periodontal/intradental receptors" proposed by Dong et al. (1993). The two theories describe the innervation systems based on different types of mechanoreceptors, but the first theory does not accept dentine sensitivity. Later studies (Pashley et al. 2002: 52, fig. 2-39) describe different mechanisms of dentine sensitivity (including both types). Accordingly, we can assume that both types of mechanoreceptor are significant in the shrew's chewing process. In addition, we also assume that periodontal sensitivity and dentine sensitivity have unequal effects in different species. Thus, one possible explanation for the difference in hard matter/pulp volume ratio may be the unequal impact of the named types. For instance, the species in which there is a relatively short distance between the anterior end of the pulp and the incisor apex (*S. mirabilis*, *N. fodiens*, *B. brevicauda*) have a well-developed system of dentine mechanoreceptors; the opposite condition (e.g., *S. minutissimus*) supposes less developed dentine mechanoreceptors and more developed periodontal ones. However, this thesis requires additional research in the future.

The phylogenetic resolving power of endodontic morphology

Currently, many zoologists investigate shrew systematics and phylogeny using molecular methods (e.g., Ohdachi et al. 2006; Dubey et al. 2007; Willows-Munro and Matthee 2009; Esteva et al. 2010; Bannikova et al. 2018, among others). Several convincing phylogenetic models of soricid evolution have been suggested during the last dozen years; all of them include the members of two modern subfamilies, Soricinae and Crocidurinae, with an extra one if the Myosoricinae Kretzoi, 1965 is considered a separate subfamily. This taxonomic limitation is associated with the specifics of the molecular methods. In contrast, traditional investigations based on morphology display broad taxonomic and age coverage (Butler 1988; Reumer 1984, 1998; Lopatin 2006) but have not yielded a phylogenetic model in terms of cladistic methodology (sensu Wiley 1981; Wiley et al. 1991; Kitching et al. 1998). Thus, we have a bias towards the development of molecular phylogenetic models that cannot be correctly compared with the nonexistent morphology-based model. The need for these comparisons requires the investigator to translate the "molecular tree" into classification, but this action is not trivial. The translation of cladistic phylogenies directly into classifications (sensu Benton 2000) is restricted by the technical possibilities for comparisons of "molecular trees" (e.g., Dubey et al. 2007) with "traditional classifications" (e.g., Reumer 1998) and has caused destabilization of the nomenclature, at least (e.g., see composition of *Crocidura* Wagler, 1832 sensu Bannikova and Lebedev 2012). Accordingly, a phylogenetic model based on morphology is required. The availability of such a model will probably permit a broader look at soricid evolution than we have now. However, such a model does not yet exist, and a significant step in its development is the identification of specific features. Our results display the applicability of endodontic morphology to phylogenetic research. We identified age-related changes in pulp volume and canal diameter, but these changes do not limit the possibility of intra- and intergroup comparisons. For instance, Fig. 5 shows several features that depend on age (reduction in pulp horn height and radicular canal diameter, for example) as well as features that are specific to individual species and are found independently of age stage (for example, the number of radicular canals and the direction in which the central canal curves). The following features (Table 1) of the pulp endocast can be used in further cladistic analyses:

Character #1: I1, anterior part of coronal pulp chamber (Quick overgrowth) *S. minutissimus* state (Fig. 4), the pulp volume of the anterior part decreases rapidly with age, at least during the immature stage; during the subsequent stages, the rate is probably reduced; (slow overgrowth) *S. mirabilis* and *N. fodiens* state, the pulp volume of the anterior part decreases slowly with age; (stable) *B. brevicauda* state, the pulp volume is the largest among the species examined; it probably has a relatively stable condition of the anterior part.

Character #2: I1, medial cusp pulp extension (Stable) *S. mirabilis* state, the extension retains pulp volume with age (Fig. 4); (closed) *S. minutissimus* and *N. fodiens* state, the modest medial cusp of I1 is present but is not expressed in the pulp endocast (probably overgrows at an early age); (absent) *B. brevicauda* state, the medial cusp of I1 absent.

Character #3: I1, cervical area expression (Expressed) *S. mirabilis*, *N. fodiens* and *B. brevicauda* state, the cervical

Table 1 The age-independent endodontic character states of the upper dentition of four species of Soricinae

Characters	*S. mirabilis* (tribe Soricini)	*S. minutissimus* (tribe Soricini)	*N. fodiens* (tribe Neomyini)	*B. brevicauda* (tribe Blarinini)
	Character states			
Character #1. I1, Anterior part of coronal pulp chamber	Slow overgrowth	Quick overgrowth	Slow overgrowth	Stable
Character #2. I1, Medial cusp pulp extension	Stable	Closed	Closed	Absent
Character #3. I1, Cervical area expression	Expressed	Unexpressed	Expressed	Expressed
Character #4. Antemolars, posterocrista (central) pulp canal condition	Buccal curving	Buccal curving	Straight	Lingual curving
Character #5. Antemolars, canal of entocingulum condition	Present	Present	Present	Absent
Character #6. Antemolars, anterior radicular canal expression	Absent	Absent	Present	Absent
Character #7. P4, protocone chamber condition	Weakly expressed	Weakly expressed	Well expressed	Well expressed
Character #8. P4, hypocone chamber condition	Weakly expressed	Weakly expressed	Well expressed	Well expressed
Character #9. P4, anterolingual radicular canal condition	Absent	Absent	Present	Present
Character #10. M1–M2, mesostyle extension condition	Smoothed	Smoothed	Protruded	split
Character #11. M1–M2, metaloph extension condition	Absent	Absent	Absent	Present
Character #12. M3, radicular canal number	Four	Three	Four	Three

area can be determined by any expressed structures (e.g., torus; see Figs. 1, 2 and 7); (unexpressed) *S. minutissimus* state, the junction of the coronal and radicular parts is not marked by any expressed or protruded structures.

Character #4: Antemolars, posterocrista (central) pulp canal condition (Straight) *N. fodiens* state, the central canal is straight (Fig. 5: c); (buccal curving) *S. mirabilis* and *S. minutissimus* state, the central canal is curved towards the buccal side (Fig. 5: a, b); (lingual curving) *B. brevicauda* state, the central canal is curved towards the lingual side (Fig. 5: d).

Character #5: Antemolars, canal of entocingulum condition (Present) *S. mirabilis*, *S. minutissimus* and *N. fodiens* state, the canal is present (Fig. 5: a–c), at least during the immature age stage; (absent) *B. brevicauda* state, the canal presents by short lingual process (Fig. 5: d).

Character #6: Antemolars, anterior radicular canal expression (Present) *N. fodiens* state, the antemolars, A1–A3, display anterior radicular canals (Fig. 5: c); (absent) *S. mirabilis*, *S. minutissimus* and *B. brevicauda* state (Fig. 5), the anterior radicular canal is absent.

Character #7: P4, protocone chamber condition (Well expressed) *N. fodiens* and *B. brevicauda* state (Fig. 6: c, d), the protocone chamber is well expressed and protruded; (weakly expressed) *S. mirabilis* and *S. minutissimus* state (Fig. 6: a, b), the chamber is weakly expressed and decreases in size to a bulge.

Character #8: P4, hypocone chamber condition (Well expressed) *N. fodiens* and *B. brevicauda* state (Fig. 6: c, d), the hypocone chamber is expressed as a flattened triangle protruding from the hypoconal flange canal; (weakly expressed) *S. mirabilis* and *S. minutissimus* state (Fig. 6: a, b), the chamber is expressed very weakly as a bulge of the hypoconal flange canal.

Character #9: P4, anterolingual radicular canal condition (Present) *N. fodiens* and *B. brevicauda* state (Fig. 6: c, d), the canal is present and is stable with age; (absent) *S. mirabilis* and *S. minutissimus* state (Fig. 6: a, b), the canal is absent.

Character #10:M1–M2, mesostyle extension condition (Protruded) *N. fodiens* state (Fig. 6: c), the extension is well protruded; the condition is probably stable with age; (smoothed) *S. mirabilis* and *S. minutissimus* state (Fig. 6: a, b), the extension is better expressed on M2 than on M1, but the pulpal volume slowly decreases with age to the bulge condition; (split) *B. brevicauda* state (Fig. 6: d), the mesostyle extension is split; the gap increases with age the gap expresses with age.

Character #11: M1–M2, metaloph extension condition (Present) *B. brevicauda* state (Fig. 6: d), the extension is present as an expressed continuation of the postprotocrista; (absent) *S. mirabilis*, *S. minutissimus* and *N. fodiens* state, the extension is absent.

Character #12: M3, radicular canals number (Four) *S. mirabilis* and *N. fodiens* state, the posterobuccal canal is present as a rudiment during the immature stage; the canal closes with age, but the fused roots of the tooth are retained; (three) *S. minutissimus* and *B. brevicauda* state, the posterobuccal radicular canal is absent.

Endodontic morphology and homology of tooth elements

The problem of mammalian tooth element homology is very closely connected with evolutionary explorations and has attracted attention during the last two centuries. The first theories were proposed by Cope (1874) and Osborn (1888) and further developed by many authorities (Gregory 1934; Butler 1941, 1978, 1985, 1990; Van Valen 1982, 1994, among others). The main approach was the analysis of paleontological

material. Luckett (1993a,b) proposed new criteria for assessing tooth homology based on the analysis of dentition ontogeny. After that, Jernvall (1995) published a monograph in which the author discussed various questions related to mammalian tooth development and the evolution of its elements using both paleontological and ontogenetic criteria. The third part of Jernvall's study, "Development of tooth shape" (Jernvall 1995: 24), attracted our attention, first regarding the possible applicability of the presence/absence of pulp crown elements to a determination of their homology ("serial homology" sensu Van Valen 1994) and secondly in the possible applicability of the topographic relations between pulp endocast elements (within the crown and radicular parts) to a determination of their developmental sequences and homology. Several authors (Pashley et al. 2002: 25; Hillson 2005: 185) stated the primary role of the predentine matrix in the crown shape formation, i.e., that the pulp endocast most closely reflects the "ontogenetically" significant relationships between the elements, at least during the immature stage. Thus, in some cases, pulp endocast analysis must be preferred, and it must always be included in the analysis of the tooth surface. In our study, the endocast is presented either by exaggerated elements (functional elements) or by smoothed elements (age-related features). The functional elements, such as the cone chambers, have different relative heights. According to Jernall's conclusions, the direction of cusp proliferation and its initiation sequence are "the main determinant of the relative cusp size" (Jernvall 1995: 26). The author also wrote (ibid.): "[…] the evolutionary recent cusp in upper molars, the hypocone, is almost always the last cusp to develop […]". Therefore, the lowest position of the hypocone chamber in molariform shrew teeth corresponds to the size/position criteria listed by Jernvall. In addition, the instability of some elements within a tooth-row can reveal the degree of reduction of the elements. This process must be reflected in the pulp endocast by the expression of more elements than are found on the tooth surface. For instance, the rudimentary radicular canal of the posterobuccal root of M3 in *S. mirabilis* makes it possible to determine the plesiomorphic state "four roots of M3" of *Sorex* Linnaeus, 1758 when the tooth surface displays only three roots.

Conclusion

The endodontic morphology of shrews is complex. Our results show that it can be used to describe additional odontological features in phylogenetic investigations of the morphological basis and the homology of the tooth elements. This list may be expanded to include specific ontogenetic studies of tooth development and pulp function. Our results revealed a gradual process of dentine formation and a corresponding decrease in pulp volume in immature and mature specimens of *S. mirabilis*. However, the analysis of age-related changes also revealed an irregularity in dentine deposition within different parts of the tooth pulp cavity. We named this irregularity "selective pulp overgrowth". This process was confirmed through analysis of other specimens of *S. minutissimus*, *N. fodiens* and *B. brevicauda*. Attempts to explain the selective overgrowth led us to address tooth pulp function. According to dentistry investigations (e.g., Pashley et al. 2002), one of the functions of pulp is dentine innervation. We assume that dentine innervation is a significant feature of soricid teeth. The complexity of the occlusal surfaces of shrew teeth, the three-dimensional mobility of dentaries and the different types of prey grasping performed by this species determine a real need of shrew dentition for tactile sensibility. This function of the pulp can determine the rate of dentine formation and the selectivity of the places of its deposition. Therefore, the pulp cavity remains open despite the high rate of shrew metabolism. In addition, the overgrowth rate, for instance, in the first upper incisor of *S. minutissimus*, also may be used in phylogenetic interpretation.

A list of twelve characters illustrates how pulp endocast morphology can be used in phylogenetic investigations. We suggest that pulp endocast analysis be included in the analysis of the tooth surface to achieve the broadest and most productive usage of tooth morphology.

Acknowledgements This study was completed within the framework of the Federal themes of the Zoological Institute no. AAAA-A19-119032590102-7 "Phylogeny, morphology, and systematics of placental mammals" and Geological Institute "Paleontological grounds for the stratigraphic scale of the upper Cenozoic of Northern Eurasia". In this study, we partly used the collection materials of the Zoological Institute of RAS (http://www.ckp-rf.ru/usu/73561/).

Funding information This study was partly funded by Project no. 19-04-00049 of the Russian Foundation for Basic Research.

Appendix 1. List of the analysed specimens

Sorex mirabilis Ognev, 1937—**ZIN 83904** (Ussuriisky Nature Reserve, Primorsky Kray, Russia; collected by M.V. Okhotina in 16.08.1968; female, sad; field number 1329); **ZIN 103204** (Primorsky Kray, Russia; ad2; field number 29; add. Information unknown).

Sorex minutissimus Zimmermann, 1780—**ZIN 98582** (Novikovo Village vicinity, Sakhalinskaya Oblast', Russia; collected by M.V. Okhotina in 14.08.1977; male, sad).

Neomys fodiens (Pennant, 1771)—**ZIN 75791** (Tumenskaya Oblast', Russia; collected by B. Kudryavtsev in 07.1984; sad; field number 38).

Blarina brevicauda (Say, 1823)—**ZIN 65805** (7 Miles NW of Stevens Point Wood Co., Wisconsin, USA; collected by Michael Gorman in 09.09.1974; male, ad1; field number 2).

Appendix 2. Anatomical directions used in the descriptions

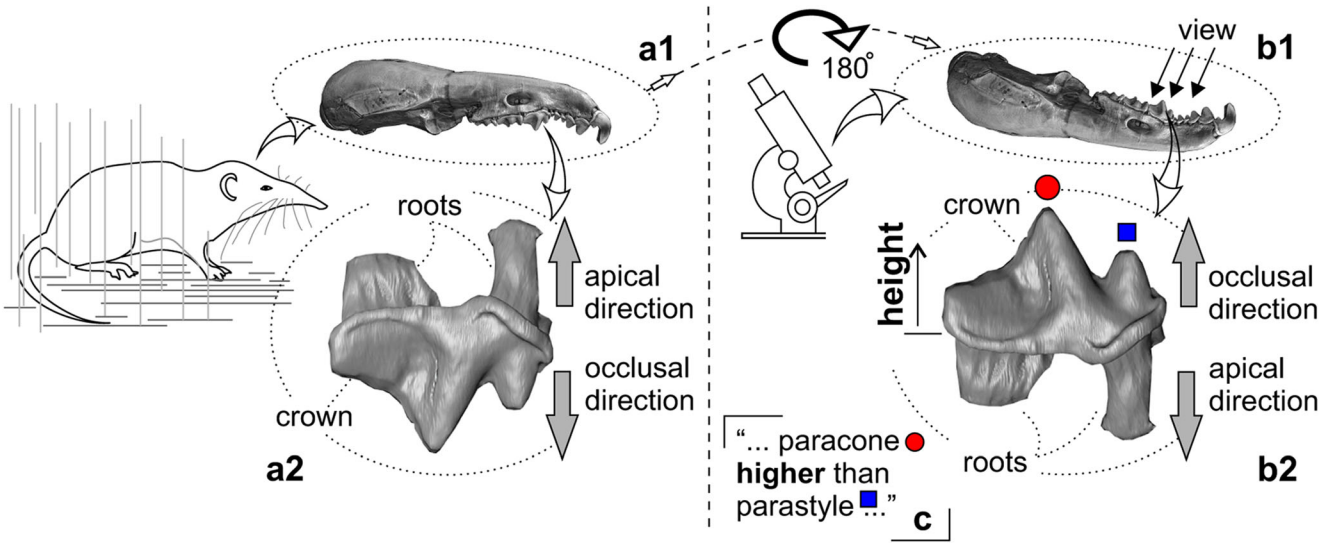

Fig. 8 Diagram showing the anatomical directions for the "natural" position of the animal (a), "reversed" position under the binocular microscope objective (b) and the part of the sentence with a correct comparative adjective (c). (a1) Shrew skull in lateral view/natural position. (a2) P4 in lateral view with the anatomical directions marked. (b1) Skull in "reversed" position with the direction of sight marked on the teeth. (b2) p4 in reversed position. (c) Correct phrase with the comparative adjective "higher". Blue quadrate, parastyle; red circle, paracone; "height", height of the crown elements (cones, styles, pulp horns, etc.)

References

Bannikova AA, Lebedev VS (2012) Order Eulipotyphla. In: Pavlinov IY, Lissovsky AA (eds) The mammals of Russia: a taxonomic and geographic reference. KMK Scientific Press, Moscow, pp 25–72

Bannikova AA, Chernetskaya D, Raspopova A, Alexandrov D, Dokuchaev N, Sheftel B, Lebedev V (2018) Evolutionary history of the genus Sorex (Soricidae, Eulipotyphla) as inferred from multigene data. Zool Scr 47:518–538

Benton MJ (2000) Stems, nodes, crown clades, and rank-free lists: is Linnaeus dead? Biol Rev 75:633–648

Borths MR, Stevens NJ (2017) Deciduous dentition and dental eruption of Hyainailouroidea (Hyaenodonta, "Creodonta," Placentalia, Mammalia). Palaentol Electron:20.3.55A: 1–20.3.55A:34

Butler PM (1941) A theory of the evolution of mammalian molar teeth. Am J Sci 239:421–450

Butler PM (1978) Molar cusp nomenclature and homology. In: Butler PM, Joysey KA (eds) Development, function and evolution of teeth. Academic Press, London, pp 439–453

Butler PM (1981) Development from the tribosphenic pattern) In: Osborn JW (ed) Dental anatomy and embryology, a composition to dental studies. Blackwell Scientific Publications, Oxford, pp 341–348

Butler PM (1985) Homologies of molar cusps and crests, and their bearing on assessments of rodent phylogeny. In: Luckett WP, Hartenberger J-L (eds) Evolutionary relationships among the rodents: a multidisciplinary approach. Plenum Press, New York, London, pp 381–401

Butler PM (1988) Phylogeny of the insectivores. In: Benton MJ (ed) The phylogeny and classification of the tetrapods, vol 2. Clarendon Press, Oxford, pp 117–241

Butler PM (1990) Early trends in the evolution of tribosphenic molars. Biol Rev 65:526–552

Byers MR, Närhi MVO (1999) Dental injury models: experimental tools for understanding neuroinflammatory interactions and polymodal nociceptor functions. Crit Rev Oral Biol Med 10:4–39

Cope ED (1874) On the homologies and origin of the types of molar teeth of Mammalia educabilia. J Acad Natl Sci Phila 8:71–91

Dong WK, Shiwaku T, Kawakami Y, Chudler EH (1993) Etatic and dynamic responses of periodontal ligament mechanoreceptors and intradental mechanoreceptors. J Neurophysiol 69:1567–1582

Dötsch C (1986) Mastication in the musk shrew, *Suncus murinus* (Mammalia, Soricidae). J Morphol 189:25–43

Dötsch C (1994) Function of the feeding apparatus in red-toothed and white-toothed shrews (Soricidar) using electromyography and cineradiography. In: Merritt JF, Kirkland GLJR, Rose RK (eds) Advances in the biology of shrews. Carnegie Institute, Pittsburg, pp 233–239

Dubey S, Salamin N, Ohdachi SD, Barrière P, Vogel P (2007) Molecular phylogenetics of shrews (Mammalia: Soricidae) revel timing of transcontinental colonization. Mol Phylogenet Evol 44:126–137

Dumont M, Tütken T, Kostka A, Duarte MJ, Borodin S (2014) Structural and functional characterization of enamel pigmentation in shrew. J Struct Biol 186:38–48

Esteva M, Cervantes FA, Brant SV, Cook JA (2010) Molecular phylogeny of long-tailed shrews (genus *Sorex*) from Mexico and Guatemala. Zootaxa 2615:47–65

Goldberg M, Lasfargues J–J (1995) Pulpo-dentinal complex revisited. J Dent 23:15–20

Goldberg M, Smith AJ (2004) Cells and extracellular matrices of dentine and pulp: a biological basis for repair and tissue engineering. Crit Rev Oral Biol Med 15:13–27

Gregory WK (1934) A half century of trituberculy the Cope-Osborn Theory of dental evolution with a revised summary of molar evolution from fish to man. Proc Am Philos Soc 73:169–317

Hill ER, Kelson KR (1959) The mammals of North America, vol 1. The Ronald Press Company, New York

Hillson S (2005) Teeth. Cambridge University Press, New York

Indra AP, Shashikala R, Nagaraj T, Santosh HN (2015) Age estimation of adults using dental pulp: a cross-sectional radiographic study. J Adv Clin Res Insights 2:131–134

Jernvall J (1995) Mammalian molar cusp patterns: developmental mechanism of diversity. Acta Zool Fenn 198:1–61

Keine M, Paul E, Sturrock CJ, Rauch C, Rutland CS (2017) Computed tomography in veterinary medicine: currently published and tomorrow's vision. Computed tomography — advanced applications. In TechOpen. http://www.intechopen.com/books/computed-tomography-advanced-applications

Kitching IJ, Forey PL, Humphries HL, Williams DM (1998) Cladistics. The theory and practice of parsimony analysis, 2nd edn. Oxford University Press, Oxford, New York, Tokyo

Klevesal GA (2007) Principles and methods of age determination of mammals. KMK Scientific Press, Moscow in Russian

Linden RWA, Millar BJ (1988) The response characteristics of mechanoreceptors related to their position in the cat canine periodontal ligament. Arch Oral Biol 33:51–56

Lopatin AV (2006) Early Paleogene insectivore mammals of Asia and establishment of the major group of Insectivora. Paleontol J 40:205–405

Luckett PW (1993a) An ontogenetic assessment of dental homologies in therian mammals. In: Szalay FS, Novacek MJ, McKenna MC (eds) Mammalian phylogeny. Mesozoic differentiation, multituberculates, monotremes, early therians and marsupials. Springer-Verlag, Berlin, pp 182–203

Luckett PW (1993b) Ontogenetic staging of the mammalian dentition, and its value for assessment of homology and heterochrony. J Mamm Evol 1:269–282

Luukko K, Kettunen P (2016) Integration of tooth morphogenesis and innervation by local tissue interactions, signaling networks, and semaphorin 3A. Cell Adhes Migr 10:618–626

Meachen-Samuels JA, Binder WJ (2009) Sexual dimorphism and ontogenetic growth in the American lion and sabertoothed cat from Rancho La Brea. J Zool 280:271–279

Morse DR, Esposito JV, Schoor RS, Williams FL, Furst ML (1991) A review of aging of dental components and a retrospective radiographic study of aging of the dental pulp and dentin in normal teeth. Quintessence Int 22:711–720

Ni X, Flynn JJ, Wyss AR (2012) Imaging the inner ear in fossil mammals: high-resolution CT scanning and 3-D virtual reconstruction. Palaentol Electron 15.2.18A:1–10

Nweeia MT, Eichmiller FC, Hauschka PV, Tyler E, Mead JG, Potter CW, Angnatsiak DP, Richard PR, Orr JR, Black SR (2012) Vestigial tooth anatomy and tusk nomenclature for *Monodon monocero*. Anat Rec 295:1006–1016

Ohdachi SD, Hasegawa M, Iwasa MA, Vogel P, Oshida T, Lin L-K, Abe H (2006) Molecular phylogenetics of soricid shrews (Mammalia) based on mitochondrial cytochrome b gene sequences: with special reference to the Soricinae. J Zool 270:177–191

Osborn HF (1888) The evolution of mammalian molars to and from the tritubercular type. Am Nat 22:1067–1079

Pashley DH, Walton RE, Slavkin HC (2002) Histology and physiology of the dental pulp. In: Ingle JI, Bakland LK (eds) Endodontics, 5th edn. B.C. Decker, Hamilton, pp 25–62

Reumer JWF (1984) Ruscinian and Early Pleistocene Soricidae (Insectivora, Mammalia) from Tegelen (the Netherlands) and Hungary. Scr Geol 73:1–173

Reumer JWF (1998) A classification of the fossil and recent shrews. In: Wójcik JM, Wolsan M (eds.) Evolution of shrews. Mammal Research Institute Polish Academy of Sciences, Białowieża, pp 5–22

Taylor JRE (1998) Evolution of energetic strategies in shrews. In: Wójcik JM, Wolsan M (eds) Evolution of shrews. Mammal Research Institute Polish Academy of Sciences, Białowieża, pp 309–346

Tumlinson R, McDaniel VR (1984) Gray fox age classification by canine tooth pulp cavity radiographs. J Wildl Manag 48:228–230

Ungar PS (2010) Mammal teeth: origin, evolution, and diversity. The John Hopkins University Press, Baltimore

Van Valen LM (1982) Homology and causes. J Morphol 173:305–312

Van Valen LM (1994) Serial homology: the crests and cusps of mammalian teeth. Acta Palaentol Pol 38:145–158

Wiley EO (1981) Phylogenetics. The principles and practice of phylogenetic systematics. Wiley & Sons, New York

Wiley EO, Siegel-Causey D, Brooks DR, Funk VA (1991) The complete cladist. A primer of phylogenetic procedure. University of Kansas Museum of Natural History, Special publication 19, Kansas

Willows-Munro S, Matthee CA (2009) The evolution of the southern African members of the shrew genus *Myosorex*: understanding the origin and diversification of a morphologically cryptic group. Mol Phylogenet Evol 51:394–398

Woods MA, Robinson QC, Harris EF (1990) Age-progressive changes in pulp widths and root lengths during adulthood: a study of American blacks and whites. Gerodontology 9:41–50

Wu X, Schepartz LA (2009) Application of computed tomography in paleoanthropological research. Prog Nat Sci 19:913–921

Zaitsev MV, Voyta LL, Sheftel BI (2014) The mammals of Russia and adjacent territories. Lipotyphlans. Izdatel'stvo "Nauka", St. Petersburg [in Russian]

Zazhigin VS, Voyta LL (2019) North Asian Pliocene-Pleistocene beremendiin shrews (Mammalia, Lipotyphla, Soricidae): a description of material from Russia (Siberia), Kazakhstan, and Mongolia and the paleobiology of Beremendia. J Paleontol. https://doi.org/10.1017/jpa.2019.51